Energy for Sustainability International Conference 2019
Designing a Sustainable Future
Turin, 24-26 July 2019

AN EQUIVALENT SELF-ADJUSTED HEAT CAPACITY METHOD FOR MODELLING HEAT DIFFUSION PROBLEMS WITH SOLID-LIQUID PHASE-CHANGE

N. Soares[1,2*], N. Rosa[1], T. Matias[3], A.G. Lopes[1], P.N. Simões[3], L. Durães[3] and J.J. Costa[1]

1: ADAI, LAETA, Department of Mechanical Engineering, University of Coimbra
Polo II Campus, Rua Luís Reis Santos
3030-788 Coimbra, Portugal
e-mail: nelson.soares@dem.uc.pt

2: ISISE, Department of Civil Engineering, University of Coimbra
Polo II Campus, Rua Luís Reis Santos
3030-788 Coimbra, Portugal

3: CIEPQPF, Department of Chemical Engineering, University of Coimbra
Polo II Campus, Rua Sílvio Lima
3030-790 Coimbra, Portugal

Keywords: Phase change material, Microencapsulated PCM, Heat diffusion, Numerical modelling, Effective heat capacity method

Abstract *This work evaluates the thermal behaviour of a small aluminium-container-based thermal energy storage (TES) unit filled with a microencapsulated phase change material (PCM) – Micronal® DS 5001 X. ANSYS CFX® software is used for the 3D numerical simulations, which are based on the Effective Heat Capacity (EHC) method considering a purely diffusive transient model. In the formulation, a new artificial self-adjusted triangular profile was considered to account for the variation of the effective specific heat with temperature. Due to the artificial nature of this procedure, the correct prediction of the phase-change kinetics was analysed. For that purpose, some previously obtained experimental data were used for validating the numerical results. The amount of stored and released energy during charging and discharging was also evaluated. The main results of this numerical study show a very good agreement with both the kinetics of the phase-change processes (average and maximum errors of 2.9 % and 11.6 %, respectively, during charging; average and maximum errors of 1.7 % and 5.0 %, respectively, during discharging) and the total amount of stored/released energy during a complete experimental charging/discharging cycle of the PCM. Moreover, it was concluded that the EHC method with a self-adjusted triangular profile to account for the variation of the effective specific heat with temperature is a good method for modelling heat diffusion problems with solid-liquid phase-change.*

1. INTRODUCTION

PCMs are very suitable for thermal management and TES applications, as they act by storing/releasing latent heat during melting/solidification in a temperature range chosen for a specific purpose [1]. The incorporation of microencapsulated PCMs into TES systems is a very attractive way to prevent problems related with liquid leakage [2–5]. Modelling thermal behaviour of microencapsulated PCMs may also become simpler as convection within microcapsules can be neglected [6,7], and the heat transfer treated as a purely diffusive problem. Microencapsulated PCMs can be mixed with other materials or encapsulated as bulk material into macrocapsules [1]. In this paper, the thermal behaviour of a small TES unit consisting of an aluminium container filled with the microencapsulated PCM is experimentally and numerically investigated. Modelling the thermal behaviour of PCMs is challenging due to the nonlinear nature of the phase-change problem [8,9] and different approaches have been used. Among them, the fixed grid EHC method has been widely used. This method introduces the concept of an equivalent heat capacity, and models the effect of the latent heat by inflating the sensible heat capacity in the whole phase-change temperature range [10]. Therefore, the heat transfer problem can be treated as a "single-phase" nonlinear conduction problem in the whole calculation domain and the governing energy equation will have the general form of the heat conduction equation with an effective specific heat (c_{eff}) varying with temperature. Therefore, the key feature of the EHC method lies in the proper definition of the c_{eff} variation profile. Typically, two ways to define this curve can be found in literature: one suggests the use of artificial c_{eff} profiles based on the properties of the PCM [11]; the other one proposes the direct use of the c_{eff} curve obtained from laboratory measurements of the effective specific heat. This paper aims to evaluate if an artificial self-adjusted triangular profile to account for the variation of c_{eff} with temperature can be used to predict the thermal behaviour of the TES unit during charging and discharging.

2. TES UNIT AND EXPERIMENTAL MEASUREMENTS

Fig. 1a shows a sketch of the TES unit used by Soares *et al.* [6,12,13]. In their experiments, several K-type thermocouples were distributed on the left (hot-surface) and right (cold-surface) faces of the TES unit, respectively, to record the time evolution of temperature on both surfaces (Fig. 1b) – $TH(t)$ and $TC(t)$, respectively. These temperatures are aimed to be considered as dynamic boundary conditions in the numerical simulations. Five K-type thermocouples were also positioned on the mid-plane of the TES unit to measure the temperature evolution within the PCM domain during the charging/discharging experiments (Fig. 1c): $T_{PCM}(t)$ was taken as the average temperature obtained from these five sensors and recorded every 30 s. Further details about the experimental setup, instrumentation and procedure can be found in refs. [6,12].

3. THERMOPHYSICAL PROPERTIES OF THE PCM

The relevant thermophysical properties of the PCM required for modelling were measured before starting the simulations (Table 1). For the aluminium, the following properties are used in the simulations: ρ = 2707 kg m^{-3}, c_p = 896 J kg^{-1} ºC^{-1} and k = 204 W m^{-1} ºC^{-1} [14].

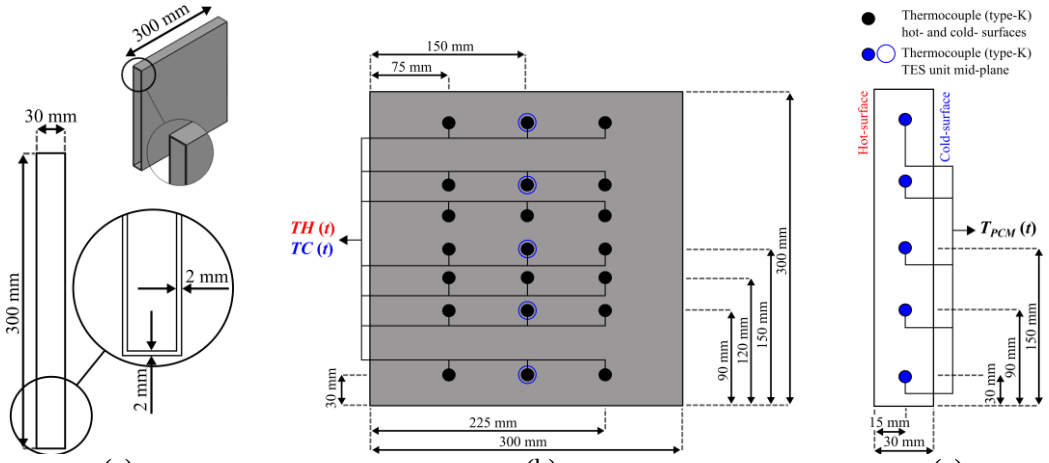

Figure 1. Sketch of the (a) physical domain of the TES unit to be filled up with the PCM; K-type thermocouples (b) on the cold- and hot-surfaces of the TES unit; (c) in the mid-plane section of the TES unit. Not to scale.

Table 1. Main thermophysical properties of the PCM Micronal® DS 5001 X – bulk PCM.

Melting peak temperature, T_m (ºC)		25.018
Solidification peak temperature, T_s (ºC)		18.914
Latent heat [10–30 ºC] (kJ kg^{-1})	− Melting, L_m	105.444
	− Solidification, L_s	99.492
Specific heat (J kg^{-1} ºC^{-1})	− Solid, c_{ps} (at 10ºC)	2408
	− Liquid, c_{pl} (at 35ºC)	1913
Thermal conductivity (W m^{-1} ºC^{-1})	− Solid, k_s	0.080
	− Liquid, k_l	0.083

4. NUMERICAL MODELLING

4.1. Effective heat capacity method

In the EHC method, the latent heat is modelled in the energy conservation equation (Eq. (1)) as an artificially inflated specific heat within the temperature interval where phase-change occurs. This high c_{eff}-value will block the increase (or decrease) of temperature during phase-change. The $c_{eff}(T)$ self-adjusted triangular profile considers that the effective specific heat represents the respective physical values in the liquid and solid phases of the PCM. In the mushy zone, in which both solid and liquid phases coexist, the PCM melted fraction (f) satisfies $0 < f < 1$. Eq. (2) presents the definition of the EHC method with the self-adjusted $c_{eff}(T)$ triangular profile for charging. The $c_{m,m}$ term given by Eq. (3) is the peak value of the equivalent specific heat, and it indicates that during phase-change the effective heat capacity of the PCM is (or grows up) directly proportional to L_m and inversely proportional to the melting temperature range, ΔT_m. T_{1m} is the temperature when the PCM begins melting and T_{2m} is the temperature for which the material is completely melted, during charging. In the EHC method, T is the only dependent variable to be solved and the method allows using the same governing equation

(Eq. (1)) for both solid and liquid phases, avoiding the need to track the melting front position to solve the problem. Indeed, the PCM melted fraction is obtained explicitly, at each time step, as a function of the computed temperature (Eq. (4), for melting process).

$$\rho \frac{\partial c_{eff} T}{\partial t} = \frac{\partial}{\partial x}\left(k \frac{\partial T}{\partial x}\right) + \frac{\partial}{\partial y}\left(k \frac{\partial T}{\partial y}\right) + \frac{\partial}{\partial z}\left(k \frac{\partial T}{\partial z}\right) \tag{1}$$

$$c_{eff}(T) = \begin{cases} c_{ps} + \dfrac{c_{m,m} - c_{ps}}{T_m - T_{1m}}(T - T_{1m}) & T_{1m} < T < T_m \\ c_{m,m} + \dfrac{c_{pl} - c_{m,m}}{T_{2m} - T_m}(T - T_m) & T_m < T < T_{2m} \end{cases}, \tag{2}$$

$$c_{m,m} = \left(2 L_m + c_{ps} \Delta T_{2m} + c_{pl} \Delta T_{1m}\right) / \Delta T_m \tag{3}$$

$$f(T) = \begin{cases} 0 & T \le T_{1m} \\ f_m\left[(T - T_{1m}) / \Delta T_{1m}\right] & T_{1m} < T < T_m \\ f_m + (1 - f_m)\left[(T - T_m)/\Delta T_{2m}\right], & T_m < T < T_{2m} \\ 1 & T \ge T_{2m} \end{cases}; \quad f_m = \frac{\Delta T_{1m}}{\Delta T_m}. \tag{4}$$

The following assumptions are also made: (*i*) conduction is the only heat transfer mechanism within the microencapsulated PCM domain; (*ii*) hysteresis of melting and solidification is taken into account by considering a ΔT_{hyst} value ($T_m > T_s$) in the problem formulation and by considering that L_m is different from L_s; (*iii*) the thermophysical properties of the materials are independent of temperature, but for the PCM c_p and k are different for the solid and liquid phases, and k varies with temperature; (*iv*) the effect of expansion/contraction of the PCM during phase-change is neglected and a constant ρ-value is used; (*v*) all materials are considered homogeneous and isotropic.

4.2. Initial and boundary conditions / monitoring variables

The boundary conditions on the left and right vertical surfaces of the numerical domain were set to be equal to the values of $TH(t)$ and $TC(t)$ measured during the experiments (Fig. 1). The top and bottom frontiers, as well as the front and back surfaces of the numerical domain were set to be adiabatic. The dimensions specified in the numerical simulations are set to be equal to those shown in Fig. 1. The times required for melting all the PCM in the numerical domain during charging, t_m, and solidifying all the material during discharging, t_s, are computed. The error over time, $ER(t)$, is also calculated. It is defined as the difference between the measured and the calculated values of T_{PCM} at each time step. The initial conditions were set to be equal to those imposed in the experiments: the charging simulation starts considering the numerical domain at 13 ºC and stops when T_{PCM} reaches 55 ºC; the discharging simulation starts considering the numerical domain at 49 ºC and stops when T_{PCM} reaches 17 ºC. The total energy stored or released by the PCM during charging or discharging, $E_{m,1}$ or $E_{s,1}$ respectively, is calculated by integrating over time the instantaneous heat rate in the aluminium-PCM interface. $E_{m,1}$ is compared to the value of the stored energy during a complete simulated charging cycle of the PCM, $E_{m,2}$, obtained from Eq. (5). $E_{m,2}$ is calculated based on the distribution of T in the PCM domain at the beginning and ending of each charging simulation. In Eq. (5), V is the volume of each control-volume occupied by the PCM; T_f and T_i are the final and initial temperatures

of the PCM at each control-volume (i,j,k), respectively. For the discharging simulations, the same procedure is considered and $E_{s,1}$ is compared to $E_{s,2}$.

$$E_{m,2} = \sum_i \sum_j \sum_k \rho_{i,j,k} V_{i,j,k} \left[c_{ps}(T_{1m} - T_i) + c_{pm}(T_{2m} - T_{1m}) + L_m + c_{pl}(T_f - T_{2m}) \right]_{i,j,k} \quad (5)$$

4.3. Numerical procedure

ANSYS CFX uses a control-volume based code with a cell-vertex finite volume, coupled implicit, pressure-based solution technique. Grid independence was declared when the variation of $E_{m,2}$ or $E_{s,2}$ between two consecutively refined grids (at a mesh refinement ratio of 1.5) was lower than 0.1 % and 0.3 %, respectively, for the charging and discharging simulations. Time-step independence was recognized when the variation of $E_{m,2}$ and $E_{s,2}$ was lower than 0.2 % and 0.5 %, respectively, considering a time-step refinement ratio of 2. Finally, a fixed regular mesh formed by 417610 nodes (control-volumes of 2 × 2 × 2 mm^3) was adopted for the calculations together with a time step of 30 s. A convergence criteria of 1×10^{-6} RMS is considered for the energy equation with domain imbalances below 1×10^{-3}. The number of iterations per time step is set as 100.

5. RESULTS AND DISCUSSION

Figs. 2a and 2b show the evolutions of $T_{PCM}(t)$ and $ER(t)$ during charging and discharging, respectively. Table 2 shows the total amount of stored and released energy computed during melting and solidification processes of the PCM. The numerical results show a very good agreement with the kinetics of the phase-change processes. In fact, a maximum error, ER, of *ca.* 11.6 % and 5.0 % was verified for charging and discharging simulations, respectively. An average error of about 2.9 % and 1.7 % was obtained for charging and discharging simulations, respectively. Moreover, the difference between the numerical and experimental values of t_m is equal to only 30 s; the difference between the numerical and experimental values of t_s is equal to 180 s. $E_{m,1}$ is only 0.1 % higher than $E_{m,2}$ and $E_{s,1}$ is only 0.1 % higher than $E_{s,2}$, which shows the robustness of the numerical procedure.

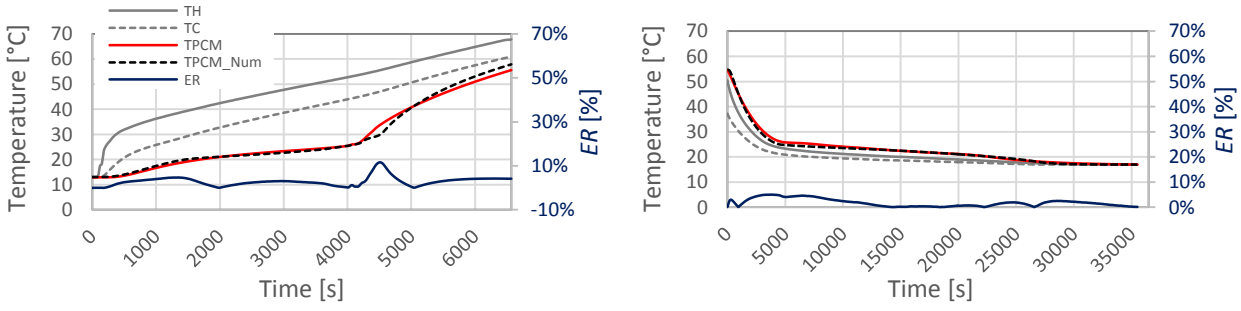

(a) (b)

Figure 2. Experimental and numerical evolutions of $T_{PCM}(t)$ and $ER(t)$ during (a) charging and (b) discharging.

Table 2. Computed variables during charging and discharging *vs.* experimental results.

Charging				Discharging			
$E_{m,1}$ (kJ)	$E_{m,2}$ (kJ)	$t_{m,numerical}$ (s)	$t_{m,experimental}$ (s)	$E_{s,1}$ (kJ)	$E_{s,2}$ (kJ)	$t_{s,numerical}$ (s)	$t_{s,experimental}$ (s)
229.3	229.0	4200	4170	197.5	197.7	21840	22020

6. CONCLUSIONS

In this work an artificial self-adjusted triangular profile for $c_{eff}(T)$ was proposed to be implemented together with the EHC method in ANSYS CFX software. The numerical results were validated against experimental data. It was concluded that the numerical procedure can be used to simulate the thermal behaviour of the TES unit filled with the PCM – Micronal® DS 5001 X during charging and discharging. Indeed, the numerical approach allowed the correct prediction of the phase-change kinetics and the accurate quantification of the stored and released energy during charging and discharging.

ACKNOWLEDGMENT

This work was supported by FEDER funds through COMPETE 2020 – POCI, and by Portuguese funds through FCT in the framework of the project "PCMs4Buildings", refs. POCI-01-0145-FEDER-016750 | PTDC/EMS-ENE/6079/2014.

REFERENCES

[1] N. Soares, J.J. Costa, A.R. Gaspar and P. Santos, "Review of passive PCM latent heat thermal energy storage systems towards buildings' energy efficiency", *Energy Build* Vol. 59, pp. 82-103, (2013).

[2] Y. Konuklu, M. Ostry, H.O. Paksoy and P. Charvat, "Review on using microencapsulated phase change materials (PCM) in building applications", *Energy Build* Vol. 106, pp. 134-155, (2015).

[3] V.V. Tyagi, S.C. Kaushik, S.K. Tyagi and T. Akiyama, "Development of phase change materials based microencapsulated technology for buildings: a review", *Renew Sustain Energy Rev* Vol. 15, pp. 1373-1391, (2011).

[4] W. Su, J. Darkwa and G. Kokogiannakis, "Review of solid–liquid phase change materials and their encapsulation technologies", *Renew Sustain Energy Rev* Vol. 48, pp. 373-391, (2015).

[5] A. Jamekhorshid, S.M. Sadrameli and M. Farid, "A review of microencapsulation methods of phase change materials (PCMs) as a thermal energy storage (TES) medium", *Renew Sustain Energy Rev* Vol. 31, pp. 531-542, (2014).

[6] N. Soares, A.R. Gaspar, P. Santos and J.J. Costa, "Experimental study of the heat transfer through a vertical stack of rectangular cavities filled with phase change materials", *Appl Energy* Vol. 142, pp. 192-205, (2015).

[7] M. Lachheb, Z. Younsi, H. Naji, M. Karkri and S. Ben, "Thermal behavior of a hybrid PCM/plaster: a numerical and experimental investigation", *Appl Therm Eng* Vol. 111, pp. 49-59, (2017).

[8] Y. Dutil, D.R. Rousse, N.B. Salah, S. Lassue and L. Zalewski, "A review on phase-change materials: mathematical modeling and simulations", *Renew Sustain Energy Rev* Vol. 15, pp. 112-130, (2011).

[9] A.A. Al-abidi, S.B. Mat, K. Sopian, M.Y. Sulaiman and A.T. Mohammed, "CFD applications for latent heat thermal energy storage: a review", *Renew Sustain Energy Rev* Vol. 20, pp. 353-363, (2013).
[10] C. Chen, H. Guo, Y. Liu, H. Yue and C. Wang, "A new kind of phase change material (PCM) for energy-storing wallboard", *Energy Build* Vol. 40, pp. 882-890, (2008).
[11] I.D. Mandilaras, D.A. Kontogeorgos and M.A. Founti, "A hybrid methodology for the determination of the effective heat capacity of PCM enhanced building components", *Renewable Energy* Vol. 76, pp. 790-804, (2015).
[12] N. Soares, A.R. Gaspar, P. Santos and J. J. Costa, "Experimental evaluation of the heat transfer through small PCM-based thermal energy storage units for building applications", *Energy Build* Vol. 116, pp. 18-34, (2016).
[13] N. Soares, "Thermal energy storage with Phase Change Materials (PCMs) for the improvement of the energy performance of buildings", PhD Dissertation in Sustainable Energy Systems. University of Coimbra, Coimbra, Portugal, (2015).
[14] Y.A. Çengal, *Heat and mass transfer: a practical approach*, McGraw-Hill, 3rd ed., (2006).